Implementation of Ambiguity-Resolved Detector for High-Precision GNSS Fault Detection

Yin, Chengyu; Teunissen, P.J.G.; Tiberius, C.C.J.M.

DOI
10.33012/2024.19786

Publication date
2024

Document Version
Final published version

Published in
Proceedings of the 37th International Technical Meeting of the Satellite Division of The Institute of Navigation (ION GNSS+ 2024)

Implementation of Ambiguity-Resolved Detector for High-Precision GNSS Fault Detection

Chengyu Yin, *Delft University of Technology*
P.J.G. Teunissen, *Delft University of Technology; Curtin University*
C.C.J.M. Tiberius *Delft University of Technology*

BIOGRAPHY

Chengyu Yin is a PhD candidate at the Delft University of Technology in the Netherlands. His current research is on carrier phase ambiguity resolution and quality control theory for high-precision GNSS positioning. He obtained his bachelor's degree in Navigation Engineering from Wuhan University in China and master's degree in Earth-Oriented Space Science and Technology from the Technical University of Munich, Germany.

Peter J.G. Teunissen is a Professor of Geodesy and Satellite Navigation at Delft University of Technology, the Netherlands, and a member of the Royal Netherlands Academy of Arts and Sciences. He has been research-active in various fields of earth observation, with current research focusing on developing theory, models, and algorithms for high-accuracy applications of satellite navigation and remote sensing systems. He is a fellow of ION and a recipient of the ION Kepler Award.

Christian C.J.M. Tiberius received the Ph.D. degree on the subject of recursive data processing for kinematic GPS surveying from the Delft University of Technology, Delft, The Netherlands, in 1998. He is currently an Associate Professor at the Geoscience and Remote Sensing (GRS) Department at Delft University of Technology. His research interests include navigation, with GNSS and terrestrial radio positioning, primarily for automotive applications.

ABSTRACT

Ambiguity resolution plays a critical role in fast and high-precision applications of the Global Navigation Satellite System (GNSS). The parameter estimation of high-precision GNSS can benefit from ambiguity resolution when its success rate is very close to 1 (e.g., larger than 0.995); otherwise it is better, in order to avoid a substantial probability of incorrect resolution, to ignore the integer property of the ambiguity, and use the float solution. Nonetheless, model validation and fault detection can still benefit from the integer property of the ambiguity with relatively low ambiguity resolution success rates (e.g. between 0.8 and 0.995) by applying the ambiguity-resolved (AR) detector test statistic based on the ambiguity-resolved residual. Due to the integer property of the resolved (so-called fixed) ambiguity estimator, the distribution of the ambiguity-resolved residual cannot be evaluated analytically. Consequently, the critical value of the AR detector has to be obtained numerically via Monte Carlo simulation of the quantile. Due to the inherent uncertainty in the Monte Carlo simulation process, the implementation of the AR detector also needs to evaluate the uncertainty associated with the simulated critical value. If the simulation uncertainty is large, the actual significance level of the detector may deviate significantly from the target value. In this study, we first describe the process of simulating the samples of the AR test statistic and obtaining the AR critical value for a given significance level through Monte Carlo simulation of the quantile. A histogram of the AR test statistic samples will be shown as an example to illustrate the irregular shape of the distribution of this test statistic. Furthermore, we introduce three methods that can be used to evaluate the uncertainty of the simulated critical value: 1) variance based on the asymptotic normality of the Monte Carlo quantile estimator, 2) confidence interval based on a distribution-free approach, and 3) variance obtained numerically by repeating the simulation. We conduct experiments to compare the above three methods in terms of the consistency between the simulation uncertainties reported by these methods. It will also be shown how the uncertainty of the critical value simulation is affected by the specified significance level. Moreover, we provide the uncertainties of the critical value simulations for nine observation models with various numbers of simulation samples and significance levels, offering insights into the number of samples that should be used for simulating the ARD critical value with the desired uncertainty when applying the AR detector.

I. INTRODUCTION

Model validation is important for GNSS data processing since observables may contain unmodeled effects and cause the assumed model to be misspecified, such as atmosphere delays and outliers due to multipath. If they remain unnoticed, the estimated parameters can be biased (Teunissen, 2017a). The first step of the model validation is typically the *detection* based on an overall model test (Baarda, 1968; Kok, 1984; Teunissen, 2000). Whether the assumed model is proper to use can be determined based on the detection outcome.

https://doi.org/10.33012/2024.19786

The GNSS mixed integer model recovers the integer property of the ambiguity vector and thus contains both real- and integer-valued unknowns (Leick et al., 2015; Teunissen and Montenbruck, 2017). The current detection methods for the GNSS mixed-integer model are based on the float or known ambiguity (Teunissen, 2024). In the ambiguity-float (AF) case, the test statistic is computed with the AF residual. The integer property of the ambiguity is ignored and does not contribute to the model validation. The ambiguity-known (AK) detector can be applied only when the ambiguity vector is given instead of estimated. In most applications, the ambiguity vector is resolved when the success rate is close to 1 (e.g., > 0.995) and consequently assumed to be a known vector. This approach is different from applying the AK detector. Ambiguity-resolved detection theory (Teunissen, 2024) has recently been developed for the GNSS mixed-integer model validation. Compared with the AF detector, the AR detector utilizes the integer property of the ambiguity vector and can provide higher detection power than the AF detector even if the ambiguity resolution success rate is not close to 1 (Yin et al., 2024). Compared with the currently used detection methods with the resolved ambiguity vector, it does not assume the ambiguity vector to be known and releases the high success rate requirement for ambiguity resolution.

Since there is no closed-form expression for the distribution of the AR test statistic, the AR critical value should be obtained numerically using Monte Carlo simulation (Teunissen, 2024). Due to the inherent uncertainty in the Monte Carlo simulation process, the implementation of the AR detector also needs to evaluate the uncertainty associated with the simulated critical value. If the simulation uncertainty is large, the actual significance level of the detector may deviate significantly from the target value. This contribution focuses on two topics regarding the implementation of the AR detector: how to evaluate the uncertainty of the simulated AR critical value and how many samples are required for the simulation to obtain a certain simulation uncertainty.

Three methods are described for the first topic: 1) variance based on the asymptotic normality of the Monte Carlo quantile estimator, 2) confidence interval based on a distribution-free approach, and 3) variance obtained numerically by repeating the simulation. We then use experiments to check the consistency between the three methods. To address the second topic, we formulate nine observation models with different dimensions of ambiguity vectors and ambiguity resolution success rates. For each model, we simulate the critical values for different significance levels with varying numbers of samples and evaluate the uncertainty of the simulations. The experiments provide insights into the number of samples that should be used to simulate the AR critical value when implementing the AR detector.

This contribution is organized as follows. In section II, we review the detection theory for the GNSS mixed-integer model and introduce how to simulate the AR critical value with an example. In section III, we describe three methods to evaluate the uncertainty of the simulated AR critical value. The three methods are compared in the first experiment in section IV. In the second experiment in section IV, we employ nine observation models and evaluate the uncertainty of the simulation for different significance levels with different numbers of samples. Finally, the summary and conclusions are provided in section V.

II. MIXED-INTEGER MODEL VALIDATION

In this section, we first review the misspecification detection theory for the GNSS mixed-integer model. Then, we introduce how the critical value of the AR detector can be simulated with Monte Carlo simulation.

1. Detection theory

The (linearized) GNSS mixed integer observation model can be written as (Leick et al., 2015; Teunissen and Montenbruck, 2017),

$$\mathcal{H}_0: \quad E\{\underline{y}\} = Aa + Bb, \quad D\{\underline{y}\} = Q_{yy}, \tag{1}$$

where $\mathcal{H}_0$ refers to the null-hypothesis; $\underline{y} \sim \mathcal{N}_m(E\{\underline{y}\}, Q_{yy})$ is the m-vector that contains the carrier phase and pseudorange observables which are assumed to be normally distributed; underscore '$\underline{\cdot}$' denotes a random vector or variable; $a \in \mathbb{Z}^n$ contains the unknown carrier phase ambiguities and $b \in \mathbb{R}^p$ contains real-valued unknowns; $[A, B]^{m\times(n+p)}$ is the design matrix of full column rank;

Two detectors currently used for detecting the misspecification in the model (1) are the ambiguity-float (AF) and ambiguity-known (AK) detectors (Teunissen, 2024). The AF detector employs the ambiguity-float residual where the integer property of the ambiguity is not considered,

$$\underline{\hat{e}} = P^{\perp}_{[A,B]}\underline{y}, \tag{2}$$

where $P^{\perp}_{M} = I - M(M^TQ^{-1}_{yy}M)^{-1}M^TQ^{-1}_{yy}$ is an orthogonal projector that projects onto the orthogonal complement of the range space of the given matrix M.

The AK detector utilizes the ambiguity-known residual where the ambiguity is a *known* integer vector and is removed from the

unknown vector,

$$\underline{\hat{e}}(a) = P_B^{\perp}(\underline{y} - Aa). \tag{3}$$

It should be noted that the AK detector can hardly be applied in practice because the ambiguity is typically *estimated* instead of deterministically known.

When ambiguity resolution is conducted, by replacing the known a in (3) with the resolved integer ambiguity vector, denoted as $\underline{\check{a}}$, we obtain the ambiguity-resolved residual,

$$\underline{\check{e}} = \underline{\hat{e}}(\underline{\check{a}}) = P_B^{\perp}(\underline{y} - A\underline{\check{a}}). \tag{4}$$

The resolved integer ambiguity $\underline{\check{a}}$ is obtained in two steps. In the first step, the integer property of the ambiguity vector is ignored, and the so-called float estimator $\underline{\hat{a}}$ and its variance-covariance (vc) matrix $Q_{\hat{a}\hat{a}}$ is computed as

$$\begin{aligned} &\underline{\hat{a}} = \left(\bar{A}^T Q_{yy}^{-1} \bar{A}\right)^{-1} \bar{A}^T Q_{yy}^{-1} \underline{y}, \;\; \bar{A} = P_B^{\perp} A, \\ &Q_{\hat{a}\hat{a}} = \left(\bar{A}^T Q_{yy}^{-1} \bar{A}\right)^{-1}. \end{aligned} \tag{5}$$

In the second step, the float ambiguity can be resolved to an integer vector, denoted as $\underline{\check{a}}$, with an integer estimator. Although there are different classes of estimators to resolve the ambiguity (Teunissen, 2017b), we restrict ourselves to the class of integer estimator in this research (Teunissen, 1999b), which resolves the float ambiguities to an integer vector. In this class of estimators, the integer least-squares (ILS) estimator has the highest success rate of resolving the float ambiguity to the correct integer (Teunissen, 1999a) and thus provides the performance closest to the ambiguity-known case. Therefore, this contribution will focus on the critical value of the AR detector using the ILS estimator to resolve the ambiguity. The LAMBDA method (Teunissen, 1995) is used to obtain the ILS solution efficiently, which conducts the integer search with the decorrelation-transformed ambiguity vector $\underline{\hat{z}}$ and its vc-matrix $Q_{\hat{z}\hat{z}}$,

$$\underline{\hat{z}} = Z^T \underline{\hat{a}}, \;\; Q_{\hat{z}\hat{z}} = Z^T Q_{\hat{a}\hat{a}} Z, \tag{6}$$

where Z^T is an admissible ambiguity decorrelation transformation matrix. The probability of resolving the float ambiguity to the correct integer is known as the success rate, which also provides a scalar measure of the precision of the float ambiguity estimator. The success rate of the ILS estimator can not be computed analytically but can be approximated by the integer bootstrapping (IB) success rate with the decorrelated ambiguity (Teunissen, 1998) since it is easy-to-compute and provides a tight lower bound (Teunissen, 1999a; Verhagen, 2003).

$$P(\check{z}_{IB} = Z^T a) = \prod_{i=1}^{n} \left[2\Phi\left(\frac{1}{2\sigma_{\hat{z}_{i|1,\cdots,n-1}}} \right) - 1 \right], \tag{7}$$

where a is the correct but unknown ambiguity, n is the dimension of the ambiguity vector; $\Phi(x) = \int_{-\infty}^{x} \frac{1}{\sqrt{2\pi}} \exp\{-\frac{1}{2}v^2\} dv$ is the cumulative distribution function (CDF) of the standard normal distribution; the conditional standard deviations $\sigma_{\hat{z}_{i|1,\cdots,n-1}}$ are the square roots of the diagonal values of the D matrix, provided by the triangular factorization $Q_{\hat{z}\hat{z}} = LDL^T$.

Based on the three types of residuals, the test statistics of the three detectors can be formulated. The AF and AK detectors test statistics, and their distributions under the null-hypothesis $\mathcal{H}_0$ are given as,

$$\begin{aligned} &\text{AF: } \|\underline{\hat{e}}\|^2_{Q_{yy}} \sim \chi^2(r, 0), \\ &\text{AK: } \|\underline{\hat{e}}(a)\|^2_{Q_{yy}} \sim \chi^2(r(a), 0), \end{aligned} \tag{8}$$

where r is the redundancy of the model with the unknown ambiguities and $r(a)$ is the redundancy of the model when the ambiguities are known, i.e., ambiguities are excluded from the unknown vector.

The AR test statistic can be written as (Teunissen, 2024)

$$\|\underline{\hat{e}}(\underline{\check{a}})\|^2_{Q_{yy}} = \|\underline{\hat{e}}\|^2_{Q_{yy}} + \|\underline{\check{\epsilon}}\|^2_{Q_{\hat{a}\hat{a}}}, \tag{9}$$

where $\underline{\check{\epsilon}} = \underline{\hat{a}} - \underline{\check{a}}$ is the ambiguity residual with the probability density function under the assumed model (1) (Teunissen, 2002)

$$f_{\underline{\check{\epsilon}}}(x) = \frac{\sum_{z \in \mathbb{Z}^n} \exp\{-\frac{1}{2}\|x + z\|^2_{Q_{aa}}\}}{\sqrt{|2\pi Q_{\hat{a}\hat{a}}|}} s_0(x), \tag{10}$$

where $s_0(x)$ is the indicator function of the integer estimators' pull-in region centered at the origin (Teunissen, 2017b).

With the corresponding test statistics, the three detectors then read

$$\begin{aligned}
&\text{AF: Reject } \mathcal{H}_0 \text{ if } \|\underline{\hat{e}}\|^2_{Q_{yy}} > \chi^2_\alpha\,(r,0)\\
&\text{AK: Reject } \mathcal{H}_0 \text{ if } \|\underline{\hat{e}}(a)\|^2_{Q_{yy}} > \chi^2_\alpha\,(r(a),0)\\
&\text{AR: Reject } \mathcal{H}_0 \text{ if } \|\underline{\hat{e}}\|^2_{Q_{yy}} + \|\underline{\check{\epsilon}}\|^2_{Q_{\hat{a}\hat{a}}} > \kappa_\alpha
\end{aligned} \tag{11}$$

where α is the user-specified significance level, and κ_α is the AR critical value, which can not be obtained analytically due to the unknown distribution of the AR test statistic; the method to obtain κ_α will be introduced in the following subsection.

2. ARD critical value simulation

The critical value of the AR detector can be obtained through Monte Carlo quantile simulation (Serfling, 1980, p.74) since there is no closed-form expression for its distribution $f_{\|\underline{\check{e}}\|^2_{Q_{yy}}}(x)$. Assuming we use N samples in Monte Carlo simulation, the AR critical value can be obtained as follows:

(i) Obtain N samples of $\|\underline{\hat{e}}\|^2_{Q_{yy}}$ according to the distribution $\chi^2\,(r,0)$, $\|\hat{e}\|^2_{Q_{yy},1}, \ldots, \|\hat{e}\|^2_{Q_{yy},i}, \ldots, \|\hat{e}\|^2_{Q_{yy},N}$.

(ii) Generate float ambiguity samples $\hat{a}_1, \ldots, \hat{a}_i, \ldots, \hat{a}_N$, that follow the normal distribution $\mathcal{N}_n(0, Q_{\hat{a}\hat{a}})$ and conduct ambiguity resolution with the LAMBDA method (Teunissen, 1995) to resolve the float ambiguity samples. Then we get samples of the resolved ambiguity, $\check{a}_1, \ldots, \check{a}_i, \ldots, \check{a}_N$.

(iii) Compute samples of the ARD test statistic with

$$\|\check{e}\|^2_{Q_{yy},i} = \|\hat{a}_i - \check{a}_i\|^2_{Q_{\hat{a}\hat{a}}} + \|\hat{e}\|^2_{Q_{yy},i}.$$

(iv) Finally, sort the samples $\|\check{e}\|^2_{Q_{yy},i}$ in ascending order, the $[(1-\alpha)N]$-th ordered sample is taken as the critical value, with $[\cdot]$ the rounding operator.

Following are several remarks on the simulation procedures. The distribution of $\check{\epsilon}$ will not change if $\underline{\hat{a}}$ is shifted by an integer vector. Therefore, we can shift the mean of the float ambiguities to zero in step (ii). Because of the independence between $\underline{\hat{e}}$ and $\underline{\check{\epsilon}}$, we can generate samples of $\|\underline{\hat{e}}\|^2_{Q_{yy}}$ and $\|\underline{\check{\epsilon}}\|^2_{Q_{\hat{a}\hat{a}}}$ independently and then obtain samples of $\|\underline{\check{e}}\|^2_{Q_{yy}}$. The LAMBDA method is used in step (ii) because we are interested in the critical value of the AR detector using the ILS estimator to resolve the ambiguity.

Fig.1 shows normalized histograms of samples generated in the simulation procedure and compares the distributions of the three test statistics. This example is created with a single-epoch short baseline double-differenced single-frequency model with 7 GPS satellites. The redundancy $r = 3$, number of ambiguities $n = 6$, and ambiguity-known redundancy $r(a) = 9$. The ILS success rate is around 84%. $N = 10^7$ samples are generated in the simulation, and the histograms are normalized to provide the probability density. In Fig.1(a), we observe the chi-squared distributed samples of $\|\underline{\hat{e}}\|^2_{Q_{yy}}$ in blue. The red curve is the distribution of $\|\underline{\hat{a}} - a\|^2_{Q_{\hat{a}\hat{a}}}$ with the known ambiguity. The histogram of $\|\underline{\check{\epsilon}}\|^2_{Q_{\hat{a}\hat{a}}}$ samples in green is different from the red curve, showing that the resolved ambiguity should not be assumed to be a known vector when applying the AR detector. Fig.1(b) compares the distributions of the three test statistics. The distribution of the AR test statistics lies between the AF and AK distributions. According to (10), the ambiguity residual is bounded inside the ambiguity pull-in region s_0. Therefore, its distribution is also bounded with zero probability density for the large values. As a result, the AR distribution is pushed towards the left compared with the AK distribution.

III. UNCERTAINTY OF SIMULATED AR CRITICAL VALUE

The critical value κ_α of the AR detector fulfills

$$\int_{-\infty}^{\kappa_\alpha} f_{\|\underline{\check{e}}\|^2_{Q_{yy}}}(x)dx = 1 - \alpha, \tag{12}$$

which is the $(1-\alpha)$-th quantile of the CDF of $\|\underline{\check{e}}\|^2_{Q_{yy}}$. As is described in subsection II.2, it is simulated by taking the $[(1-\alpha)N]$-th ordered sample of the AR test statistic, denoted as $\hat{\kappa}_\alpha$, which is an order statistic from the distribution $f_{\|\underline{\check{e}}\|^2_{Q_{yy}}}(x)$.

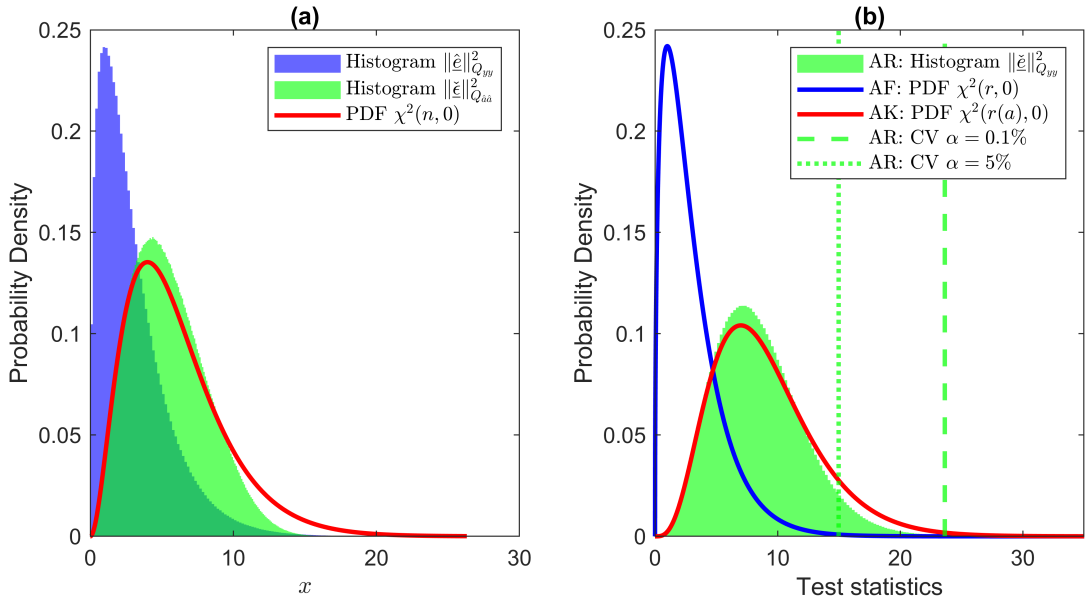

Figure 1: (a) Normalized histograms of samples of $\|\underline{\hat{e}}\|^2_{Q_{yy}}$ in blue and $\|\underline{\check{e}}\|^2_{Q_{\hat{a}\hat{a}}}$ in green (b) Distributions of the AF test statistic in blue, AR test statistic in green, and AK test statistic in red. AR critical values for $\alpha = 0.1\%$ and 5% are shown in dashed lines in green

Before describing three methods to evaluate the uncertainty of the simulated AR critical value $\hat{\kappa}_\alpha$, we introduce the distribution of order statistics, the theoretical foundation to quantify simulation uncertainty.

1. Order statistics

Order statistics (Serfling, 1980, p.87) are the ordered i.i.d. (independent and identically distributed) samples following a certain PDF $f(x)$ (the corresponding CDF is $F(x)$). N i.i.d. ordered samples $x^{(k)} \sim f(x)$ can be written as,

$$x^{(1)} \leq x^{(2)} \leq \cdots \leq x^{(k)} \leq \cdots \leq x^{(N)}. \tag{13}$$

According to this definition, the simulated AR critical value $\hat{\kappa}_\alpha$ is the $[(1-\alpha)N]$-th order statistic from N samples of $f_{\|\underline{\check{e}}\|^2_{Q_{yy}}}(x)$.

The exact CDF of the k-th sample $x^{(k)}$, $P(x^{(k)} \leq x)$, can be derived in two steps. First, it can be split as

$$P\left[x^{(k)} \leq x\right] = \sum_{i=k}^{N-1} P\left[x^{(i)} \leq x < x^{(i+1)}\right] + P\left[x^{(N)} \leq x\right]. \tag{14}$$

Then, the individual probabilities in (14) can be obtained based on the Binomial distribution with i successes in N independent Bernoulli trials with success probability $F(x)$,

$$P\left[x^{(i)} \leq x < x^{(i+1)}\right] = \binom{N}{i} [F(x)]^i [1-F(x)]^{N-i} \tag{15}$$

Finally, the CDF of $x^{(k)}$ can be obtained by substituting (15) into (14),

$$P\left[x^{(k)} \leq x\right] = \sum_{i=k}^{N} \binom{N}{i} [F(x)]^i [1-F(x)]^{N-i}, -\infty < x < \infty \tag{16}$$

The PDF of the order statistic $x^{(k)}$ can be derived by differentiating the CDF (Casella and Berger, 2002, p.229),

$$f_{x^{(k)}}(x) = \frac{N!}{(k-1)!(N-k)!} f(x) [F(x)]^{k-1} [1-F(x)]^{N-k}. \tag{17}$$

In a special case, when $x^{(k)} \sim U(0,1)$, with $U(0,1)$ the standard uniform distribution, i.e., $f(x) = 1, F(x) = x$,

$$f_{x^{(k)}}(x) = \frac{N!}{(k-1)!(N-k)!} x^{k-1} (1-x)^{N-k}, 0 < x < 1. \tag{18}$$

Thus, the k-th order statistic from $U(0,1)$ has a beta distribution beta$(k, N-k+1)$. It will be shown later that although we do not have the closed-form expression of $f_{\|\underline{\check{e}}\|^2_{Q_{yy}}}(x)$, we can still obtain a confidence interval of the critical value simulation based on (18).

2. Method-I: asymptotic approach based on order statistics

The asymptotic normality of the simulated AR critical value $\hat{\kappa}_\alpha$ is written as (Serfling, 1980, p.77)

$$\hat{\kappa}_\alpha \sim AN\left(\kappa_\alpha,\ \sigma^2_{\hat{\kappa}} = \frac{1}{N} \cdot \frac{\alpha(1-\alpha)}{f^2_{\|\underline{\check{e}}\|^2_{Q_{yy}}}(\kappa_\alpha)}\right) \tag{19}$$

where AN refers to an asymptotic normal distribution. When the number of samples in the simulation approaches infinity, $\hat{\kappa}_\alpha$ will follow a normal distribution with κ_α mean and variance equals $\sigma^2_{\hat{\kappa}}$ in (19). Therefore, $\hat{\kappa}_\alpha$ is a *consistent* estimate of κ_α and its variance can be approximated with $\sigma^2_{\hat{\kappa}}$.

In practice, $f^2_{\|\underline{\check{e}}\|^2_{Q_{yy}}}(\kappa_\alpha)$ is unknown. It can be estimated from the samples by the probability density at $\hat{\kappa}_\alpha$. After that, a confidence interval can be obtained based on the above asymptotic variance.

Eq. (19) shows that the variance of the simulation is proportional to $\alpha(1-\alpha)$ and inversely proportional to the number of samples N and the probability density at the critical value. Table 1 shows an example to compare the uncertainty of the AR critical value simulation for different significance levels. The observation model in this example is the same as that used for Fig.1. When the significance level increases from 0.1% to 5%, $\alpha(1-\alpha)$ increases from around 0.001 to 0.0475, while the probability density at the critical value also increases significantly, as is shown in the table and Fig.1(b). As a result, the standard deviation of the simulated critical value decreases from 0.0208 to 0.0034. With the same observation model and the number of samples, the critical value for $\alpha = 5\%$ can be simulated more precisely than that of $\alpha = 0.1\%$.

	$\alpha = 0.1\%$	$\alpha = 0.5\%$	$\alpha = 1\%$	$\alpha = 5\%$
$\hat{\kappa}_\alpha$	23.625	20.166	18.641	14.971
$\alpha(1-\alpha)$	0.0010	0.0050	0.0099	0.0475
$f_{\|\underline{\check{e}}\|^2_{Q_{yy}}}(\kappa_\alpha)$	0.0005	0.0024	0.0046	0.0203
$\sigma_{\hat{\kappa}}$	0.0208	0.0094	0.0068	0.0034

Table 1: Uncertainty of AR critical value simulation for different significance levels for $N = 10^7$

3. Method-II: distribution-free confidence interval

Method-I is based on the asymptotic distribution and the probability density $f_{\|\underline{\check{e}}\|^2_{Q_{yy}}}(\kappa_\alpha)$. Method-II can obtain a confidence interval without the information of the underlying distribution (Serfling, 1980, p.102).

Assume we have N i.i.d. ordered samples follow $f_{\|\underline{\check{e}}\|^2_{Q_{yy}}}(x)$, and the $(1-\alpha)$-th quantile $\hat{\kappa}_\alpha = x^{(k)}$. The probability that the correct but unknown critical value κ_α lies in the interval $\left[x^{(i)}, x^{(j)}\right]$ is

$$\begin{aligned} P\left[x^{(i)} < \kappa_\alpha < x^{(j)}\right] &\overset{*}{=} P\left[F(x^{(i)}) < F(\kappa_\alpha) < F(x^{(j)})\right] \\ &\overset{**}{\approx} P\left[\hat{F}(x^{(i)}) < F(x^{(k)}) < \hat{F}(x^{(j)})\right] \\ &= P\left[i/N < F(x^{(k)}) < j/N\right] \end{aligned} \tag{20}$$

* CDF of the AR critical value $\|\underline{\check{e}}\|^2_{Q_{yy}}$ is written as $F(x)$ for simplification, which is monotonically increasing.

** $F(x^{(i)})$ is approximated by $\hat{F}(x^{(i)})$ obtained from samples, which equals i/N. κ_α is replaced by its simulation $x^{(k)}$.

Since $x^{(k)}$ is a sample that follows the CDF $F(x)$, $F(x^{(k)})$ follows the standard uniform distribution $U(0,1)$, and it can be interpreted as the k-th order statistic in N samples following $U(0,1)$. Therefore, according to (18), $F(x^{(k)}) \sim \text{beta}(k, N-k+1)$.

The last step is to choose proper indexes i and j to obtain the confidence interval. For example, for a confidence interval of probability p, i and j can be chosen according to $P\left[F(x^{(k)}) < i/N\right] \approx (1-p)/2$ and $P\left[F(x^{(k)}) > j/N\right] \approx (1-p)/2$. Then, i and j can be computed with the inverse of the beta CDF.

4. Method-III: repeating simulation

The uncertainty can also be evaluated empirically by repeating the simulation multiple times and computing the empirical variance. The number of repetitions N_r can be 50 and 100 (Morio and Balesdent, 2015; El Masri et al., 2021). Assume we use N samples to simulate the AR critical value and repeat the simulation for N_r times.

- At each time, N samples are used for simulation, and the simulated critical value is denoted as $\hat{\kappa}_\alpha^i$, $i = 1, \ldots, N_r$.
- The empirical variance of $\hat{\kappa}_\alpha$ simulated with N samples can then be computed as the variance of the repetitions $\hat{\kappa}_\alpha^i$.

Method III requires more computational effort than methods I and II since the simulation should be run for N_r times. It is still a very useful method because methods I and II may provide unreliable uncertainty when the number of samples is small. The asymptotic normality (19) used in method I holds only if the number of samples N is infinity, which is impossible in practice. Moreover, it is based on the probability density at the critical value approximated from the samples. Eq (19) can be a good approximation only when N is very large. The confidence interval obtained with method II is based on the simulated CDF $\hat{F}$ and the simulated critical value $\hat{\kappa}_\alpha = x^{(k)}$; thus, the probability inside this confidence interval is not exactly equal to the probability p. Method III can provide reliable uncertainty for the simulation even with small numbers of samples if the number of repetitions N_r is large enough, e.g., 50 and 100.

IV. EXPERIMENT

1. Compare three methods for uncertainty evaluation

To compare the uncertainty of the simulated AR critical value obtained from the three methods, we generate confidence intervals using the variances computed with method I and method III by assuming the simulated critical value follows a normal distribution, which can then be compared with the confidence interval obtained with method II.

Fig.2 (left) compares the 99% confidence interval obtained with the three methods with a single-frequency GPS model, the same model used for the example in Fig.1. Fig.2 (right) compares the 99% confidence interval with a short-baseline double-differenced dual-frequency GPS model with 9 GPS satellites. The redundancy $r = 13$, number of ambiguities $n = 16$, and ambiguity-known redundancy $r(a) = 29$. The ILS success rate is around 99%. The AR critical values for four significance levels are simulated with 10^6 samples and the ILS estimator. The reference AR critical values shown by horizontal lines in red are simulated with $N = 5 \times 10^7$ samples. The asterisks in the middle give the simulated critical value, and the error bar provides the 99% confidence interval. It is shown in Fig.2 that the confidence intervals created with the three methods have similar ranges in both the single-frequency and dual-frequency experiments. The reference critical values are covered in all the 99% confidence intervals.

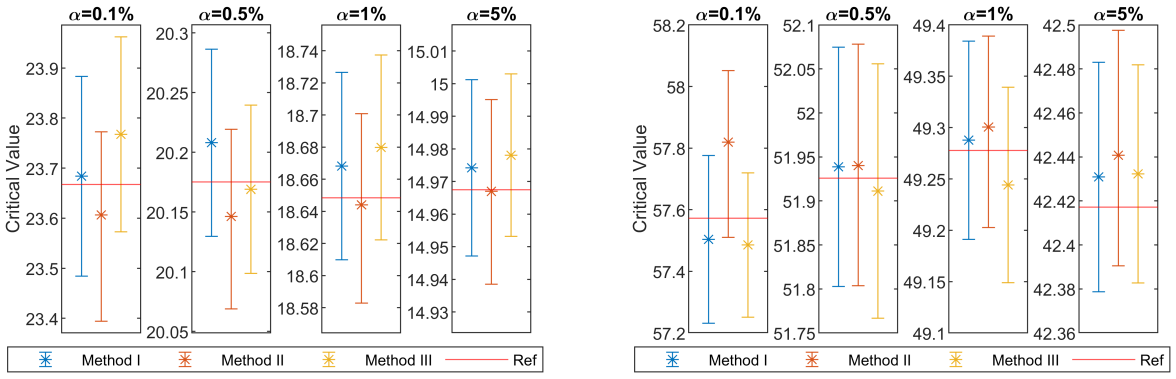

Figure 2: Compare 99% confidence intervals obtained with three methods. Left figure is based on a single-frequency GPS model and right figure is based on a dual-frequency GPS model. The critical values for four significance levels are simulated with $N = 10^6$ samples, and the reference critical values shown in red are simulated with $N = 5 \times 10^7$ samples.

Fig.3 shows the confidence intervals obtained with smaller numbers of samples. Fig.3 (left) uses $N = 10^5$ samples and Fig.3 (right) uses $N = 5 \times 10^5$ samples to simulate the critical values. This example is based on the same singe-frequency model as that of Fig.2 (left). The confidence intervals in Fig.3 (left) can be different from each other, especially for $\alpha = 0.1\%$ and $\alpha = 0.5\%$. The confidence intervals in Fig.3 (right) are more consistent because more samples are used. As we discussed in section III.4, method III can be used for simulations with small numbers of samples, in which case methods I and II are unreliable. Fig.3 shows that with $N = 10^5$ samples, methods I and II can not be used for $\alpha = 0.1\%$ and $\alpha = 0.5\%$. For $N = 5 \times 10^5$ samples, they are acceptable for all the significance levels we tested.

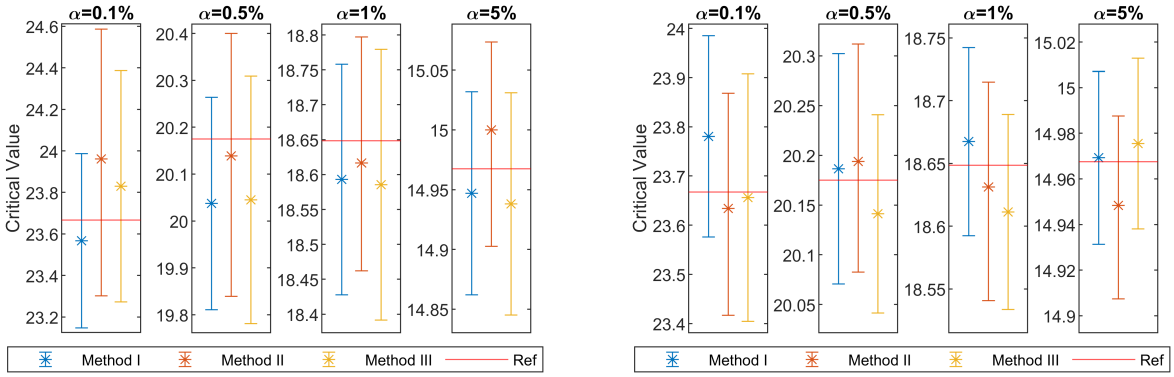

Figure 3: Compare 99% confidence intervals obtained with three methods with single-frequency GPS observation model. $N = 10^5$ samples are used in left figure and $N = 5 \times 10^5$ samples are used in right figure. Reference critical values in red are simulated with $N = 5 \times 10^7$ samples.

2. Simulation uncertainty and number of samples

We conduct experiments to investigate the relation between the number of samples and the uncertainty of the simulation, which will provide insights into how many samples should be used to simulate the critical value when applying the AR detector. The experiments in this subsection are based on nine single-epoch short-baseline double-differenced observation models with ambiguity vectors of different dimensions and ambiguity resolution success rates. Details of these models can be found in Table 2, including the dimension of the ambiguity vector n, ambiguity resolution success rate, number of satellites, and the AF model redundancy r. We simulate critical values with these models for $\alpha = [0.1\%, 0.5\%, 1\%, 5\%]$ and numbers of samples $N = [10^4, 5 \times 10^4, 10^5, 5 \times 10^5, 10^6]$. The 99% confidence intervals are formulated for all the simulations with the variances obtained through method III by assuming that $\hat{\kappa}_\alpha$ follows a normal distribution. The AR critical values are simulated with the ILS estimator to resolve the ambiguities.

Models	Frequency	n	Success Rate	#Satellites	r
1	L1	6	83%	7	3
2	L1	6	88%	7	3
3	L1	7	93%	8	4
4	L1	8	99%	9	5
5	L1+L2	10	83%	6	7
6	L1+L2	10	89%	6	7
7	L1+L2	12	96%	7	9
8	L1+L2	12	99%	7	9
9	L1+L2+L5	15	99%	6	12

Table 2: Observation models for experiments

Fig.4 shows 99% confidence intervals of the AR critical values simulated with different numbers of samples N and significance levels α. The dots in the middle give simulated critical values, and error bars provide 99% confidence intervals. Horizontal lines give the corresponding reference critical values simulated with $N = 5 \times 10^7$ samples. Confidence intervals are based on the variances obtained by repeating the simulations for 50 times (Method III). Confidence intervals cover the corresponding reference critical values in all the experiments, demonstrating that Method III provides a reliable variance for the critical value simulation. For the same number of samples, the critical value for larger α can be simulated more precisely, which agrees with what we discussed in Table 1. For the critical value of $\alpha = 0.1\%$ (in blue), the confidence intervals are loose when N is smaller than 5×10^5, while for $\alpha = 5\%$ (in green), the critical value can be simulated with good precision with 5×10^4 samples.

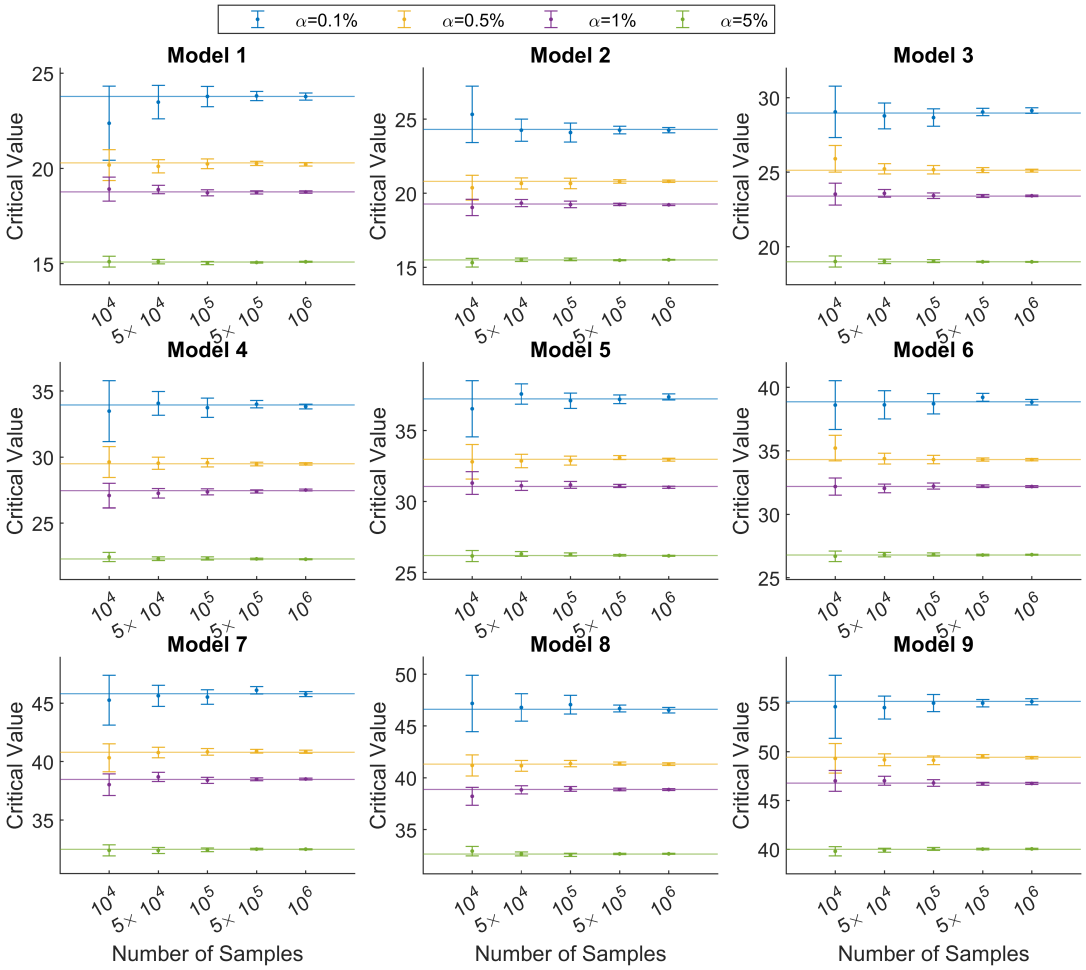

Figure 4: 99% confidence intervals of AR critical values simulated with $N = [10^4, 5 \times 10^4, 10^5, 5 \times 10^5, 10^6]$ samples for different significance levels, indicating by different colors. Dots in middle give simulated critical values, and error bars provide 99% confidence intervals. Horizontal lines give corresponding references simulated with $N = 5 \times 10^7$ samples. Confidence intervals are obtained based on repeating simulations 50 times (Method III).

Fig.4 provides the uncertainty of the simulated critical values $\hat{\kappa}_\alpha$, but it does not show what will be the impact on the actual significance level of the detection when $\hat{\kappa}_\alpha$ is used. In practice, a critical value is chosen to fulfill the user-specified significance level. It is useful to obtain a confidence interval for the significance level provided by the simulated $\hat{\kappa}_\alpha$ because it can provide uncertainty information in the domain of the significance level. The confidence interval in the domain of the significance level is obtained as follows. According to,

$$P\left[CI_L < \kappa_\alpha < CI_U\right] = p \tag{21}$$

with CI_L and CI_U the lower and upper bounds of the confidence interval and p the probability that the confidence interval covers the true value, it can be written that

$$P\left[1 - F(CI_L) > 1 - F(\kappa_\alpha) > 1 - F(CI_U)\right] = P\left[\alpha_L > \alpha > \alpha_U\right] = p \tag{22}$$

with $F(x)$ the CDF of the critical value; α_L and α_U the significance levels corresponding to CI_L and CI_U. By obtaining α_L and α_U, we formulate a confidence interval for the significance level corresponding to the simulated $\hat{\kappa}_\alpha$.

Based on the confidence intervals shown in Fig.4, we conduct Monte Carlo simulations to obtain α_L and α_U that correspond to the lower and upper bounds of the confidence intervals for $\hat{\kappa}_\alpha$. Simulations are carried out with 5×10^7 samples, and the uncertainty of the simulated α_L and α_U are not considered. The results, 99% confidence interval for the significance levels, are shown in Fig.5. The dashed horizontal lines in red indicate $\pm 10\%$ ranges around the specified significance levels α. The error bars give the confidence intervals, and the error bars' colors indicate the corresponding number of samples in the simulation.

The label of the horizontal axis gives the models used in the experiments.

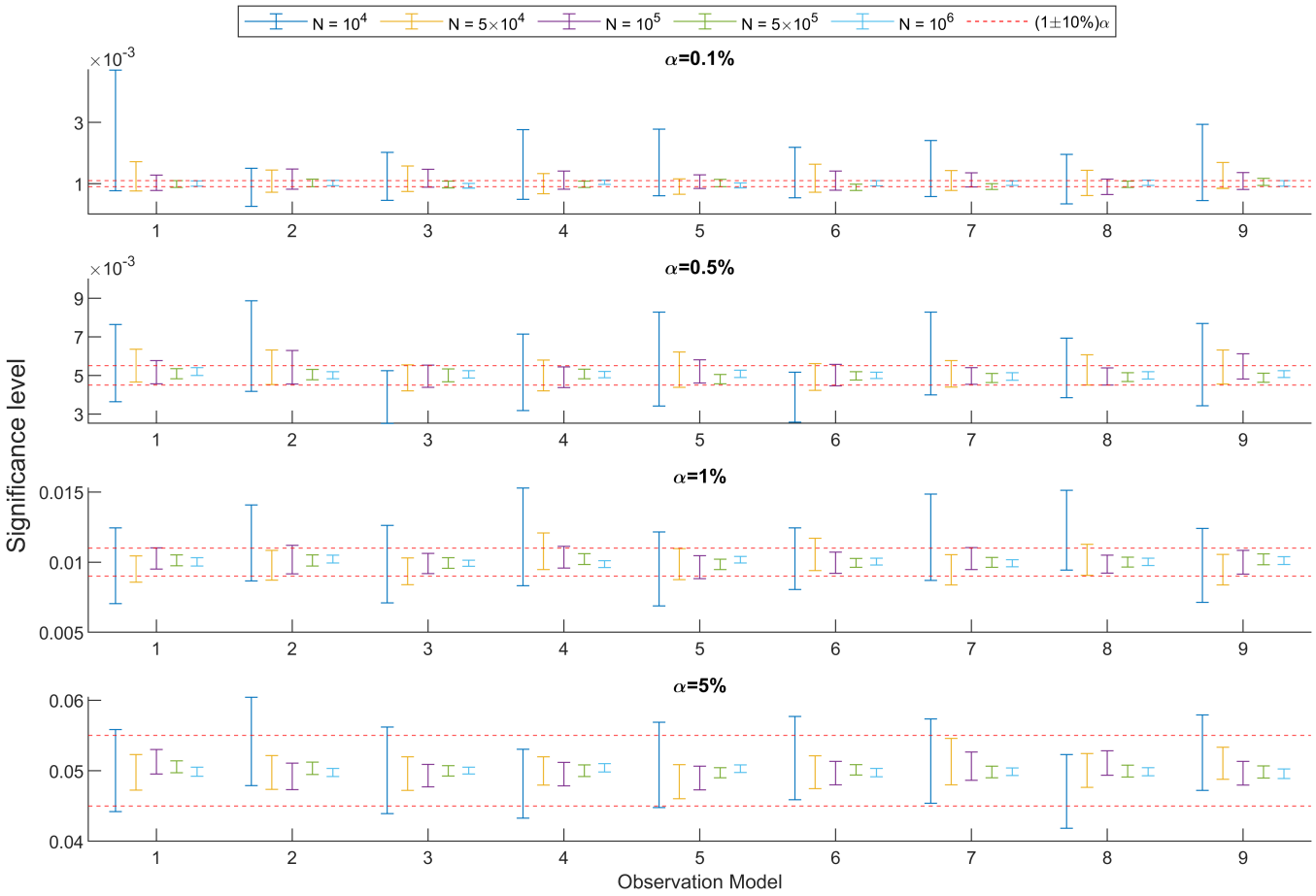

Figure 5: Confidence intervals of significance level provided by $\hat{\kappa}_\alpha$ computed based on (22). The four subplots are for different significance levels, error bars show confidence intervals, and colors indicate numbers of samples that correspond to simulations. Dashed horizontal lines in red indicate $\pm 10\%$ ranges around specified significance levels α.

As is shown in Fig.5, for the same significance level and the number of samples, ranges of the confidence intervals for different models are at a similar magnitude. The range of the confidence interval decreases with the increasing of the number of samples. For $\alpha = 0.1\%$, $N = 5 \times 10^5$ samples (in green) are needed to ensure the simulated critical value provides a significance level within the $\pm 10\%$ range around $\alpha = 0.1\%$ (between red dashed lines). For $\alpha = 0.5\%$, simulations with 10^5 samples (in purple) provide confidence intervals close to the $\pm 10\%$ range in most experiments. For $\alpha = 1\%$, simulations with $N = 5 \times 10^4$ samples (in yellow) can provide a confidence interval close to the $\pm 10\%$ range, and $N = 10^5$ samples (in purple) can ensure the confidence interval within the $\pm 10\%$ range in most experiments. For $\alpha = 5\%$, the critical value simulated with $N = 10^4$ samples (in blue) can provide a confidence interval slightly larger than the $\pm 10\%$ range. With $N = 5 \times 10^4$ samples (in yellow), the precision will be better, and the confidence intervals are much narrower than the $\pm 10\%$ range. Therefore, to make the simulated AR critical value (with the ILS estimator) provide a significance level of approximately $\pm 10\%$ around the specified one, the number of samples should be used for $\alpha = 0.1\%, 0.5\%, 1\%, 5\%$ are $N = 5 \times 10^5, 10^5, 5 \times 10^4, 10^4$, respectively.

V. SUMMARY AND CONCLUSIONS

In this contribution, we discussed several topics related to the implementation of the ambiguity-resolved (AR) detector. The critical value of the AR detector should be obtained by Monte Carlo simulation. We introduced three methods to evaluate the uncertainty of the simulated critical value, conducted experiments to compare these three methods, and provided insights into the number of samples that should be used to simulate the AR critical value.

We first reviewed the detection theory for the GNSS mixed-integer observation model and introduced the procedure to simulate the AR critical value using the Monte Carlo simulation. We exhibited the distributions and histograms related to the AR test

statistic and showed that the resolved ambiguity should not be assumed as a known vector when applying the AR detector.

Then, we introduced how to evaluate the uncertainty of the simulated AR test statistic κ_α. We described the distribution of the order statistic and three methods to obtain variances and confidence intervals of κ_α, including an asymptotic approach based on order statistics, a distribution-free confidence interval, and obtaining the variance by repeating the simulation. Based on the asymptotic normality of κ_α, we showed how the simulation uncertainty decreased with the significance level α increasing from 0.1% to 5%.

In the experiment part, we first compared the three methods to evaluate the uncertainty of $\hat{\kappa}_\alpha$. We found that the three methods were consistent when the number of samples $N \geq 5 \times 10^5$ and were inconsistent for $\alpha = 0.1\%$ and $\alpha = 0.5\%$ when $N = 10^5$ because method I and method II could not provide precise approximations of the uncertainty when the numbers of samples were small. For the simulations with small numbers of samples N, Method III can be used to evaluate the uncertainty, and it requires heavy computation effort since the simulation needs to be repeated N_r times with $N \times N_r$ samples used in total. After that, we conducted numerical experiments to provide insights into the number of samples that should be used when applying the AR detector with the ILS estimator. The experiments were carried out with nine double-differenced observation models for $\alpha = [0.1\%, 0.5\%, 1\%, 5\%]$ with different numbers of samples. For the same significance level and the number of samples, the ranges of confidence intervals for different models are at a similar magnitude. In order to simulate the AR critical value that provides a significance level of approximately $\pm 10\%$ around the specified one, the number of samples should be used for $\alpha = 0.1\%, 0.5\%, 1\%, 5\%$ are $N = 5 \times 10^5, 10^5, 5 \times 10^4, 10^4$, respectively.

ACKNOWLEDGEMENTS

Chengyu Yin's work in the 'I-GNSS positioning for assisted and automated driving' project (18305) is funded by the Dutch Research Council (NWO). For this research, the Dutch national e-infrastructure Snellius supercomputer was used with the support of the SURF Cooperative using grant no. EINF-7002.

REFERENCES

Baarda, W. (1968). A testing procedure for use in geodetic networks. Technical report, Netherlands Geodetic Commission, Publ. on Geodesy, New Series, Vol. 2(5), Delft.

Casella, G. and Berger, R. (2002). *Statistical inference*. Duxbury, Pacific Grove, US.

El Masri, M., Morio, J., and Simatos, F. (2021). Improvement of the cross-entropy method in high dimension for failure probability estimation through a one-dimensional projection without gradient estimation. *Reliability Engineering & System Safety*, 216:107991.

Kok, J. J. (1984). *On data snooping and multiple outlier testing*, volume 30. US Department of Commerce, National Oceanic and Atmospheric Administration.

Leick, A., Rapoport, L., and Tatarnikov, D. (2015). *GPS satellite surveying*. John Wiley & Sons.

Morio, J. and Balesdent, M. (2015). *Estimation of rare event probabilities in complex aerospace and other systems: a practical approach*. Woodhead publishing.

Serfling, R. J. (1980). *Approximation theorems of mathematical statistics*. John Wiley & Sons.

Teunissen, P. J. G. (1995). The least-squares ambiguity decorrelation adjustment: a method for fast GPS integer ambiguity estimation. *Journal of Geodesy*, 70:65–82.

Teunissen, P. J. G. (1998). Success probability of integer GPS ambiguity rounding and bootstrapping. *Journal of Geodesy*, 72:606–612.

Teunissen, P. J. G. (1999a). An optimality property of the integer least-squares estimator. *Journal of Geodesy*, 73:587–593.

Teunissen, P. J. G. (1999b). The probability distribution of the GPS baseline for a class of integer ambiguity estimators. *Journal of Geodesy*, 73:275–284.

Teunissen, P. J. G. (2000). *Testing theory: an introduction*. VSSD Delft.

Teunissen, P. J. G. (2002). The parameter distributions of the integer GPS model. *Journal of Geodesy*, 76:41–48.

Teunissen, P. J. G. (2017a). Batch and recursive model validation. In Teunissen, P. J. G. and Montenbruck, O., editors, *Springer Handbook of Global Navigation Satellite Systems*, chapter 24, pages 687–720. Springer.

Teunissen, P. J. G. (2017b). Carrier phase integer ambiguity resolution. In Teunissen, P. J. G. and Montenbruck, O., editors, *Springer Handbook of Global Navigation Satellite Systems*, chapter 23, pages 661–685. Springer.

Teunissen, P. J. G. (2024). The ambiguity resolved detector: A new detector for the mixed-integer GNSS model. *Journal of Geodesy (accepted)*.

Teunissen, P. J. G. and Montenbruck, O. (2017). *Springer Handbook of Global Navigation Satellite Systems*. Springer.

Verhagen, S. (2003). On the approximation of the integer least-squares success rate: which lower or upper bound to use. *Journal of Global Positioning Systems*, 2(2):117–124.

Yin, C., Teunissen, P. J. G., and Tiberius, C. C. J. M. (2024). Performance of ambiguity-resolved detector for GNSS mixed-integer model. *GPS Solutions (submitted)*.